VI. APPENDIX

A. Object Pose Predictor Architecture

The architecture of our pose predictor is shown in Fig. 6. The pose predictor first extracts a 128-dimensional feature from the history buffer, and then the look-ahead time is appended to this feature, passed together through another fully-connected network to get the final predicted pose. We choose not to use recurrent architectures such as long short-term memory (LSTM) to achieve faster inference time, such that we can compute the whole predicted trajectory for the predictable range in parallel. We also tried a Transformer [47] architecture, but it does not outperform the current version based on fully-connected networks. We reach the same conclusion as stated in [48], which highlights that the Transformer architecture may not outperform in time-series forecasting tasks.
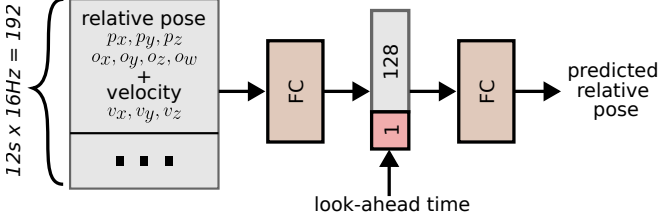

Fig. 6. **Object pose predictor architecture.** The sequence of past poses and velocities is sampled from the past 12 seconds at 16Hz. The first FC (fully-connected) network extracts a 128-dimensional feature, and the second FC network generates the predicted pose from the extracted feature and look-ahead time. All poses are relative to the previous pose.

B. Trajectories and Objects

How the 4 types of trajectories are parameterized and the set of selected objects are shown in Fig. 7. θ specifies the counter-clockwise angle of the trajectory, r is the distance from the trajectory to the robot arm base, l is the length of the trajectory (for rectangular and sinusoidal trajectories, l is the straight distance from start to end), and $d \in \{+1, -1\}$ indicates the direction of the motion, where $+1$ means counter-clockwise and -1 means clockwise. The speed v of the motion is randomly sampled but remains constant through an episode.

We select this set of objects to include both concave and convex shapes and also to ensure that the size of the object fits in the gripper. The sampling range of each trajectory parameter is shown in Table II. We design these ranges such that at least part of the trajectory is reachable for the robot arm, assuming no obstacles.

Trajectory	θ	r (m)	l (m)	d	v (cm/s)
Linear	$[0°, 360°]$	$[0.35, 0.65]$	1	$\{+1, -1\}$	$[2, 6]$
Sinusoidal	$[0°, 360°]$	$[0.35, 0.65]$	1	$\{+1, -1\}$	$[2, 6]$
Rectangular	$[0°, 360°]$	$[0.35, 0.65]$	1	$\{+1, -1\}$	$[2, 6]$
Circular	$[0°, 360°]$	$[0.65, 0.9]$	1.5	$\{+1, -1\}$	$[5, 10]$

TABLE II
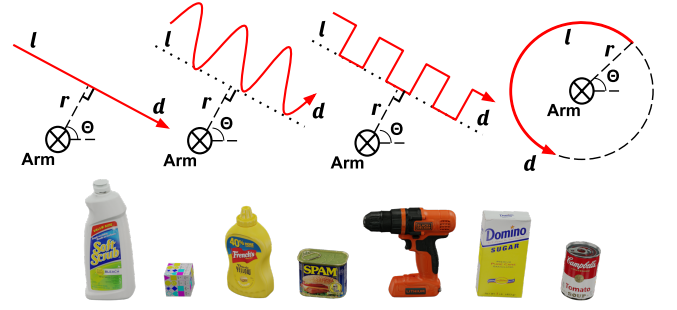PARAMETER SAMPLING RANGE FOR EACH CONVEYOR TRAJECTORY.

Fig. 7. **Randomized trajectories and selected graspable objects.** Top Row: A bird's eye view of linear, sinusoidal, rectangular, and circular conveyor belt motion generation process. Each random motion is parameterized by angle θ, distance r, length l, and direction d. The cross indicates the position of the robot base. The red line shows the motion of the conveyor belt, with an arrow indicating the direction. The horizontal dashed line at the robot base indicates the positive x-axis of the world frame. Bottom row: 7 objects from the YCB dataset are selected as the graspable target objects for our experiments.

C. Meta-controller Training Plot

The training plot with 5 random seeds of our meta-controller is shown in Fig.8.
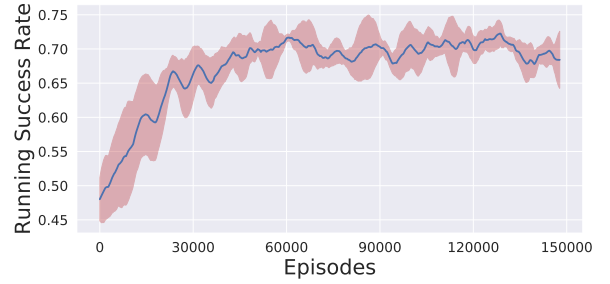

Fig. 8. **Meta-controller training plot.** Our meta-controller is trained up to 150,000 episodes (around 24 hours) with 5 random seeds. We visualize the mean of the running success rate over the past 1000 episodes and 1 standard deviation is shaded.

D. Computing Reachability

This section describes how the *Online-reachability* baseline computes the reachability value. Given a time-budget T_T, to compute the reachability of a particular predicted pose, it attempts to plan a motion towards that pose M times. t_i denotes the motion planning time for the i-th attempt. Then the reachability value R is computed as

$$R = 1 - \frac{\sum_{i=1}^{M} t_i}{MT_T}, \ 0 < t_i \leq T_T$$

When all the attempts fail, namely, the entire time budget is used up, then the reachability value of that pose is 0.

E. Comparison with Different Fixed Meta-parameters

We further compare our method to *Grid-search* on different fixed look-ahead times and time budgets in the *3-6 Random Blocks* and *Cluttered Household*, as shown in Fig. 9. We keep one of the meta-parameters in the optimal pair and then vary the other. These results show how different fixed meta-parameters can significantly impact performance. However, our meta-controller outperforms all fixed values by

modulating the meta-parameters at different iterations, based on the scene information. The gap is further exacerbated when the environment becomes more cluttered as we go from *3-6 Random Blocks* to *Cluttered Household*.

under realistic timing. Time spent in all submodules is compensated with the target object motion and we retime the planned arm motion to make sure it matches the real-robot speed.
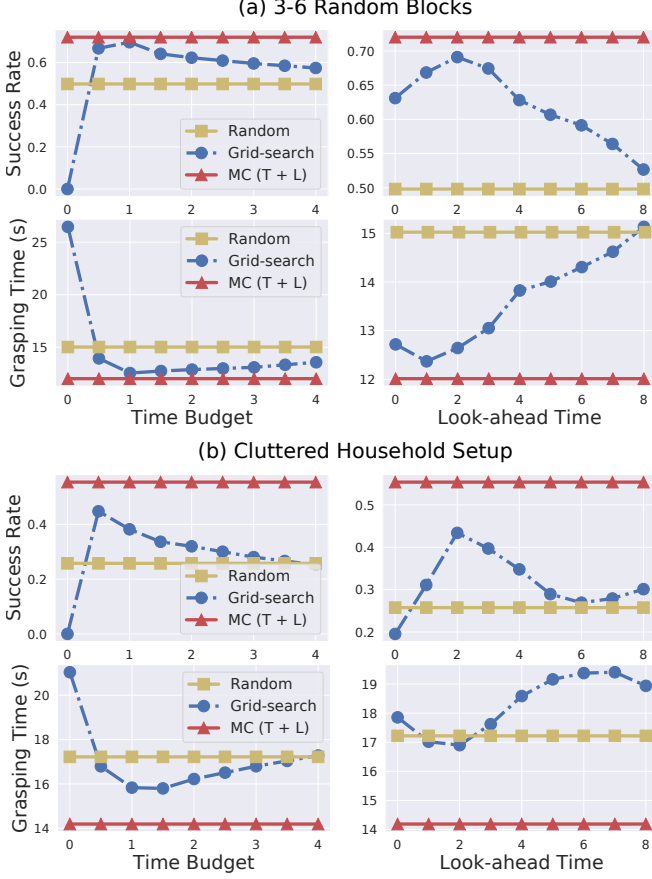

Fig. 9. **Comparison with different fixed meta-parameters in *Grid-search*.** (a) *3-6 Random Blocks*. (b) *Cluttered Household*. For each setup: the top row is the success rate, and the higher is better. The bottom row is the grasping time, and the lower is better. Each number is averaged over 2,000 trials. Our meta-controller outperforms both *Random* and *Grid-search*, and the gap becomes more significant as the environment becomes more cluttered and challenging.

F. Limitations

We are not able to provide real-world experiments. However, we think that the sim2real gap of this work is minimal, and the performance gain from the meta-controller will be consistent regardless of the sim2real gap. There are several reasons for it. (1) The largest gap when transferring to the real robot is the vision system that estimates the object poses and bounding box dimensions. Recent perception systems such as DOPE [49] and Gen6D [50] can obtain such information fast and reliably. We also add significant Gaussian noises to the poses and bounding box dimensions to account for such perception errors. Given the same magnitude, pure random noise is more challenging than noise from realistic perception systems with fixed observation-to-noise mapping. (2) Given the estimated poses and bounding box dimensions, there is no sim2real gap in other components of our pipeline, such as object pose predictor, grasp planner, motion planner, and the meta-controller. (3) Our simulated environment is